



**HAL**  
open science

# Synthesis of unlayered graphene from carbon droplets: In stars and in the lab

Phil Fraundorf, Tristan Hundley, Melanie Lipp

► **To cite this version:**

Phil Fraundorf, Tristan Hundley, Melanie Lipp. Synthesis of unlayered graphene from carbon droplets:  
In stars and in the lab. 2019. hal-02238804

**HAL Id: hal-02238804**

**<https://hal.science/hal-02238804>**

Preprint submitted on 1 Aug 2019

**HAL** is a multi-disciplinary open access archive for the deposit and dissemination of scientific research documents, whether they are published or not. The documents may come from teaching and research institutions in France or abroad, or from public or private research centers.

L'archive ouverte pluridisciplinaire **HAL**, est destinée au dépôt et à la diffusion de documents scientifiques de niveau recherche, publiés ou non, émanant des établissements d'enseignement et de recherche français ou étrangers, des laboratoires publics ou privés.

## Synthesis of unlayered graphene from carbon droplets: In stars and in the lab\*

P. FRAUNDORF,<sup>1,2</sup> TRISTAN HUNDLEY,<sup>1</sup> AND MELANIE LIPP<sup>3</sup>

<sup>1</sup>*University of Missouri StL Physics & Astronomy*

*William L. Clay Center for Nanoscience Bldg St. Louis MO 63121, USA*

<sup>2</sup>*Washington University Physics Department, St. Louis MO 63110, USA*

<sup>3</sup>*Institute for Modelling Hydraulic and Environmental Systems (IWS),  
Universität Stuttgart, Pfaffenwaldring 61, 70569 Stuttgart, Germany, EU*

### ABSTRACT

Micron-sized presolar particles from meteorite Murchison show isotopic evidence of formation from freshly made carbon atoms, around asymptotic giant branch stars. These include graphite-rimmed particles with and without a spherical core of *apparently intergrown* graphene. The origin of this unlayered material (with a density near that of graphite) was a puzzle, since sp<sup>2</sup> carbon often shows layering (e.g. 0.34 nanometer spacing in electron diffraction or images) even when nearly amorphous. We show that such core-rim particles can be grown in a laboratory evaporating carbon oven, where the cores likely condense as supercooled droplets of carbon liquid that solidify slowly enough for intergrowth of graphene sheets. Sheet coherence widths from 1 to 2 (compared to 4) nanometers in our first homemade cores suggest solidification times shorter than for the presolar case. The observations point the way to simulating astrophysical carbon vapor condensation, setting the stage for more laboratory experiments. The temperatures and pressures needed to grow supercooled liquid droplets suggest that the core-rim particles formed in third dredge-up eruptions at the photosphere base, rather than in external stellar winds. This presolar material may already have unprecedented properties in blocking diffusion, although synthesizing increased coherence-width sheets in the lab remains a challenge.

*Keywords:* carbon condensation, AGB atmospheres, unlayered graphene

### 1. INTRODUCTION

When water emerges from the gas phase in cold air, it often emerges as either snowflakes or as frozen droplets known as hail. When carbon emerges from the gas phase, polycyclic aromatic hydrocarbon "snowflakes" have been observed in a number of astrophysical environments (Tielens 2008). In warmer settings, just as with hail on earth, the vapor may also emerge as liquid droplets which freeze, but in carbon's case if these are large they may be difficult to detect by remote sensing. Of course, carbon has its own set of unusual properties.

At low and ambient pressures, solid carbon sublimates to carbon vapor when temperature rises above 3900K, so liquid carbon (like liquid CO<sub>2</sub>) is not stable at low and terrestrial-ambient pressures. However, carbon vapor may condense as liquid first on cooling, and remain supercooled before solidifying (in the absence of container walls or nucleation seeds) as do metallic liquids (Kelton & Greer 2010). This is supported by laboratory laser ablation studies of Kasuya et al. (2002) and Heer et al. (2005). If this liquid is cooled slowly to form graphene sheets, however, the isotropic (e.g. 2.5) proximity of atoms in the liquid will likely suppress the 3.4 graphite layering. Evidence of such layering is, however, ubiquitous in sp<sup>2</sup> carbons found on earth, even when nearly amorphous.

A form of sp<sup>2</sup> carbon with density approaching that of graphite but without evidence of layers (referred to hereafter as unlayered graphene) is, however, found in the interior of micron-sized presolar (Lugaro 2005) core-rim carbon spheres (Bernatowicz et al. 1996; Fraundorf & Wackenhut 2002; Croat et al. 2005, 2014), having likely formed by condensation,

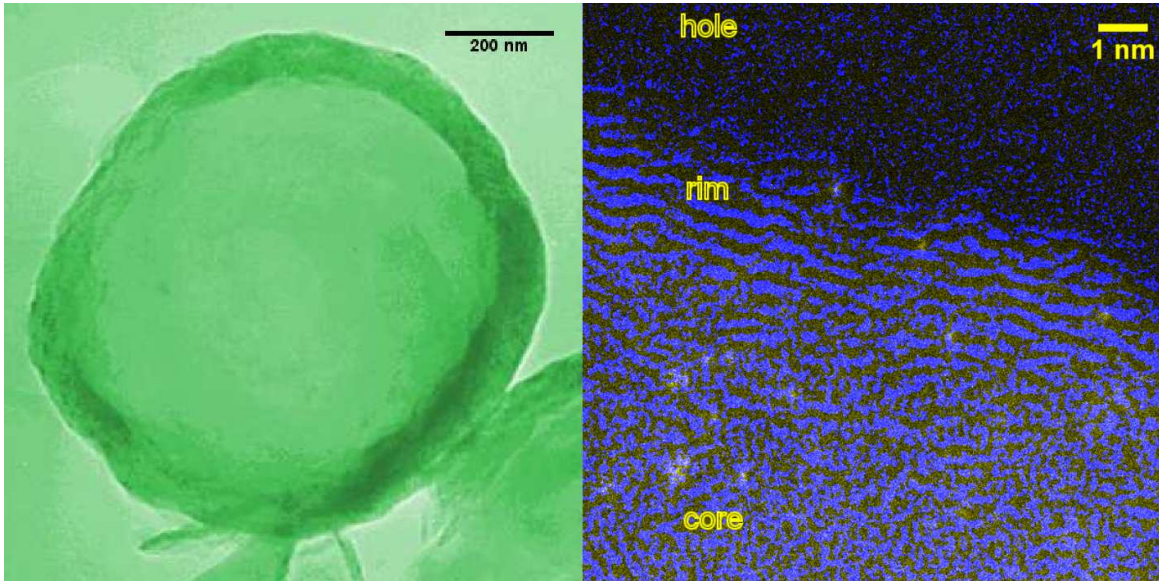


**Figure 1.** Presolar core-rim particles: Left - Brightfield transmission electron microscope (TEM) image of a presolar core-rim onion in false color to improve contrast; Right - Aberration-corrected closeup of a rim/core (top/center) interface from Oak Ridge National Lab (taken with the Pennycook Lab’s Andrew Lupini and Jing Tao) of a blue-channel brightfield showing rim (002) layers edge-on near the top, and the red/green-channel high angle annular darkfield image showing individual heavy atom nuclei in rim and core. Yellow dots show scattering from single atomic nuclei heavier than carbon, with spatial resolution  $<1\text{\AA}$ .

slow cooling, and 2D crystallization of liquid carbon droplets in the atmosphere of asymptotic giant branch stars after third dredge-up. The core itself appears to have a density comparable to (albeit perhaps a bit less than) that of graphite (Bernatowicz et al. 1996; Fraundorf et al. 2010), with an abrupt transition from core to graphite rim (Fig. 1). Lattice imaging of edge-on graphene sheets often shows intersecting line segments, suggesting that some sheets may be faceted pentacones (Mandell 2007) Here we show that such unlayered graphene cores and core-rim spheres can also be synthesized from carbon vapor in laboratories on earth, provided that steps are taken to slow down small-particle cooling (from a condensation temperature in the 3000K range) by radiative losses to a surroundings at room temperature.

## 2. EXPERIMENTAL

To do this we fabricated closed and resistively-heated carbon ovens about 6mm in outside diameter, with an open volume between 2 and 6 mm in depth and a flat separable collection surface inside, so that vapor condensed therein will be shielded from the room-temperature world outside the oven (Lipp et al. 2017; Hundley & Fraundorf 2018). Half-dozen anneals running for several minutes, with less than 200W of power, produced graphite onions with and without spherical cores with diameters in the 0.1 to 0.4 micron size range (cf. Fig. 2). The rims on some of the core-rim particles appeared to be more compact than those on the graphite-only particles, and the smaller sizes (compared to the 0.5 to 2 micron size of typical meteoritic onions) made it easier to characterize these particles without slicing via microtome. Not present (or at least not identified) in the presolar collections, we also found rim-free i.e. core-only particles.

## 3. ANALYSIS

Analysis of a selected area electron diffraction pattern from a core-rim particle in the left half of Fig. 3 shows the expected (002) spacing from the graphitic rim, as well as unexpectedly strong (hk0) spacings with high frequency tails. These tails are consistent with diffraction from unlayered graphene in the core (which constitutes about 60% of the particle by volume), but are also expected (at lower intensity) from random-layer-lattice graphite in the rim. To avoid the problem of rim diffraction, we also examined diffraction patterns from core-only particles like that in Fig. 3b. Here we saw only the (hk0) spacings expected from unlayered graphene. The graphene sheet 100 and 110 coherence widths, inferred by comparing them to Debye scattering profiles (Warren 1969) as well as using the Warren model (Warren 1941; Warren & Bodenstein 1966), were around 2 nm if the (hk0) peaks in that core-rim particle were mostly from



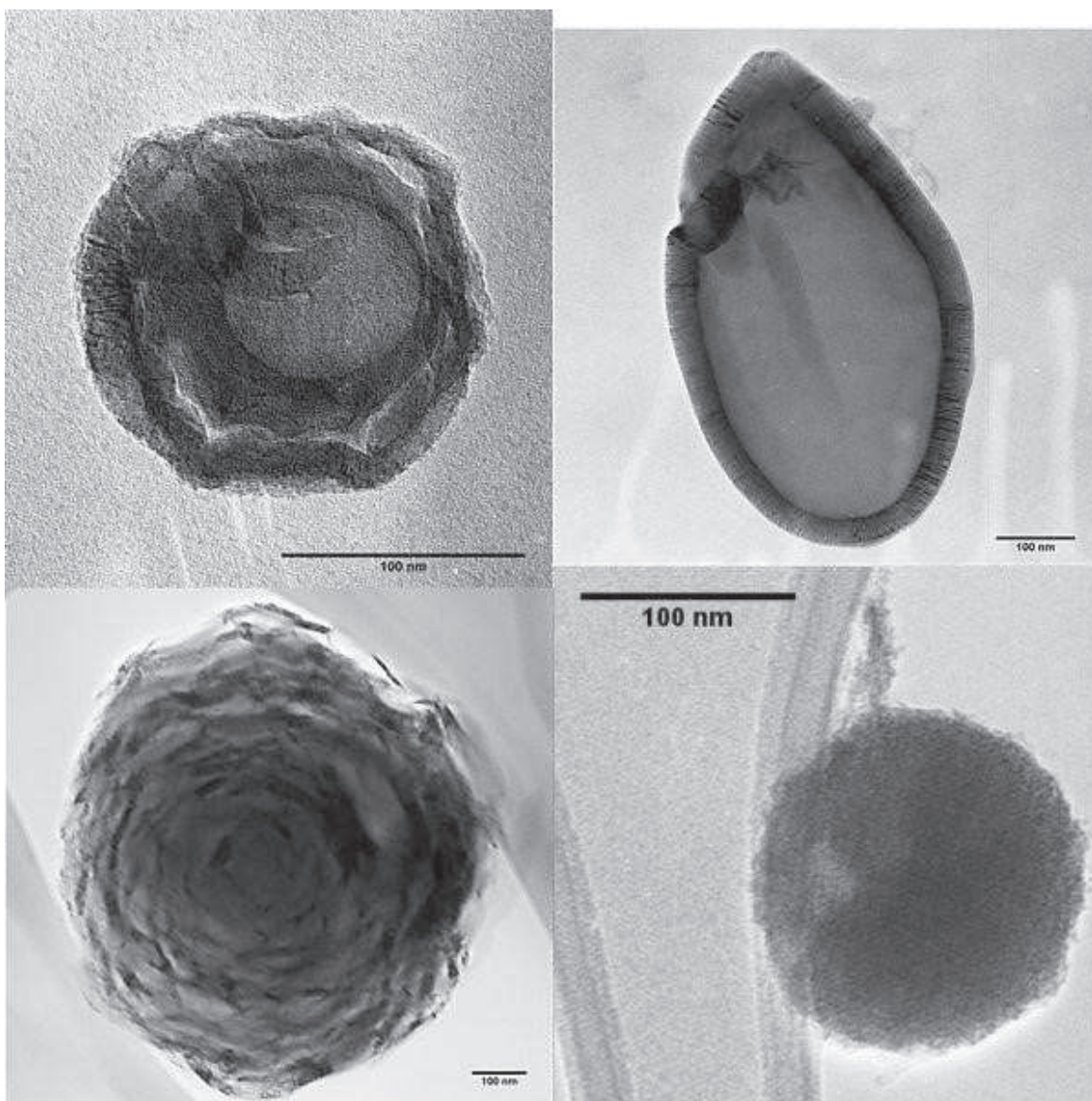


**Figure 2.** "Homegrown" particles - At top are core-rim onions, one small and another oval in shape; At bottom are a rim-only graphite onion (left) and unlayered-graphene core-only particle (right).

the core, and between 1nm and 2nm in the core-only particles, significantly smaller than the 3-4 nm coherence widths (Bernatowicz et al. 1996; Fraundorf & Wackenhut 2002) from presolar cores.

The (often complete) absence of graphite (002) spacings in both electron diffraction and HRTEM images of the presolar cores is the signature of unlayered graphene, given that even evaporated carbon viewed as amorphous often shows a diffuse (002) band. These observations are consistent with the possibility graphene-mediated solidification of a carbon liquid, nucleated on hexagonal and pentagonal loops, is a plausible mechanism for preventing graphite's 3.4 Angstrom wide van der Waals layers, and for growing unrelaxed single-walled pentacones from a 5 carbon loop seed. The weaker diffraction peaks and smaller coherence widths of graphene sheets in the homegrown cores suggest that much slower cooling rates may be needed to approach the unlayered-graphene sheet sizes and abundances found in presolar core-rim particles.

Although the evaporating oven approach described here also shows promise for decreasing the cooling rate within the 3000K range, and for adding other molecules to a simulated stellar atmosphere, the control of cooling rate in the experiments reported here was limited. It's quite possible, given that only parts of each oven were hot enough to evaporate carbon, that radiative cooling times from 3300K to 2800K for a 100 nm particle were in the tens of

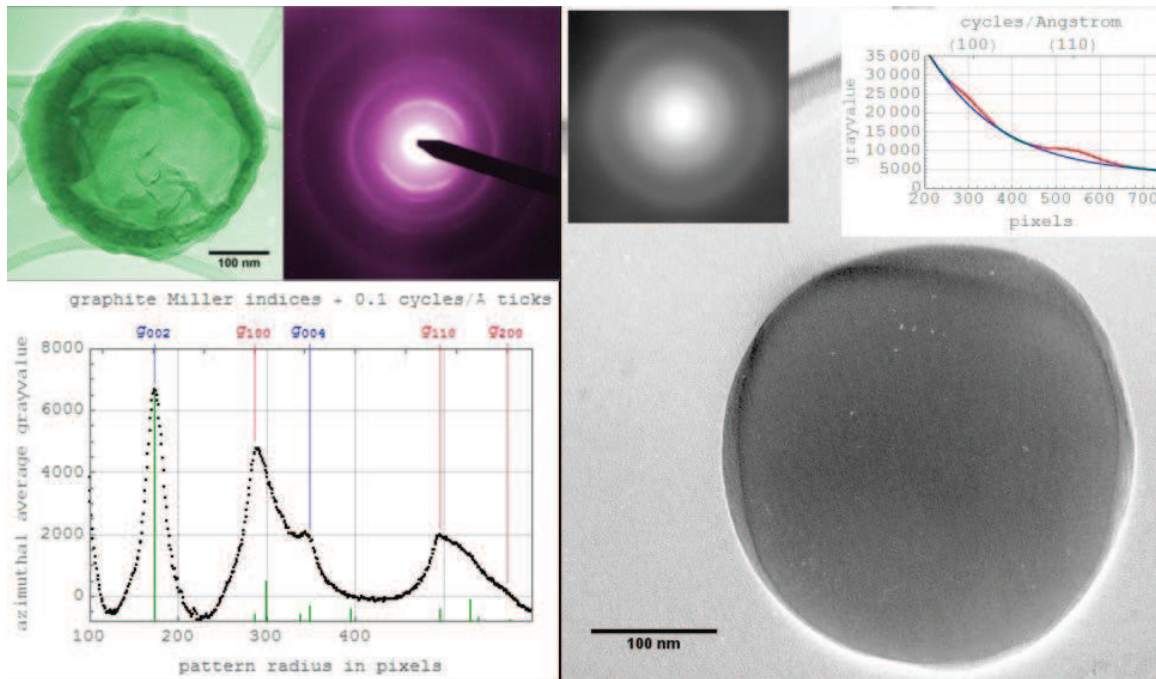


**Figure 3.** Left half - Brightfield TEM image at top of a graphite particle from our third annealing run, a selected area diffraction pattern of the whole particle at top right, and a background subtracted azimuthally-averaged profile analysis at bottom; Right half - at top left a selected area diffraction pattern of the core-only particle shown at bottom, and an azimuthally-averaged profile showing broad graphene-only peaks.

microseconds rather than the millisecond range (an upper limit on this oven design set by gravitational settling in a vacuum).

#### 4. DISCUSSION

About carbon's behavior, nucleation as liquid is expected if the melting temperature drops below the sublimation line (depending on pressure) for particle diameters below 2nm (Yang & Li 2008). The results further suggest, however, that the containerless maximum supercooling temperature, typically above 50% of the melting temperature (Kelton & Greer 2010), for liquid carbon at low pressure may be lower than the 70% to 90% observed experimentally e.g. for close-packed (12 nearest neighbor) metals. This is consistent with earlier cited reports of evidence for droplet formation in the absence of attempts at shielding from rapid radiative heat loss (Kasuya et al. 2002; Heer et al. 2005), and also consistent with the "rearrangement cost" (Kelton & Greer 2010) likely when going from e.g. an icosahedral (12 nearest neighbor) carbon liquid to a more densely packed (3 nearest neighbor) unlayered graphene. Given a carbon triple point in the 4800K range (Bundy et al. 1996; Savvatimskiy 2015), as shown in Fig. 4, this still puts the likely containerless droplet solidification temperature for liquid carbon above 2400K.

About synthesis in cool giant stars, as is the case for presolar carbon particles showing graphite rims about a carbide seed (Bernatowicz et al. 1996, 2005), possible trajectories on Fig. 4 for formation of particles showing graphite rims about unlayered graphene cores will require regions of "relatively high" carbon vapor density (e.g. clumps and/or jets) for droplet precipitation, growth, and solidification compared to the lower-temperature regions e.g. found in spherically-symmetric wind-driven stellar outflows (Wasserburg et al. 1995; Bernatowicz et al. 1996; Lodders & Fegley 1997; Bernatowicz et al. 2005). In addition for these graphite-rim/core particles, the problems with growth rate and temperature are exacerbated if particle cores must grow into the half-micron size range (as in Fig. 1) before the transition from supercooled liquid to intergrown graphene. Thus the formation-region for these graphite-rim/core particles is both hotter, and higher in carbon vapor-pressure, than that discussed by Lodders & Fegley (1997) for the particles with graphite rims on carbide seeds.

As shown in Fig. 4, in addition to the need for higher pressures and temperatures, oxygen's tendency to tie up carbon atoms in gaseous form suggests that core-rim particle formation will require an O/C ratio less than 1/4 (Lodders & Fegley 1997). This, along with the C12/C13 enrichments seen in these particles relative to stellar photo-

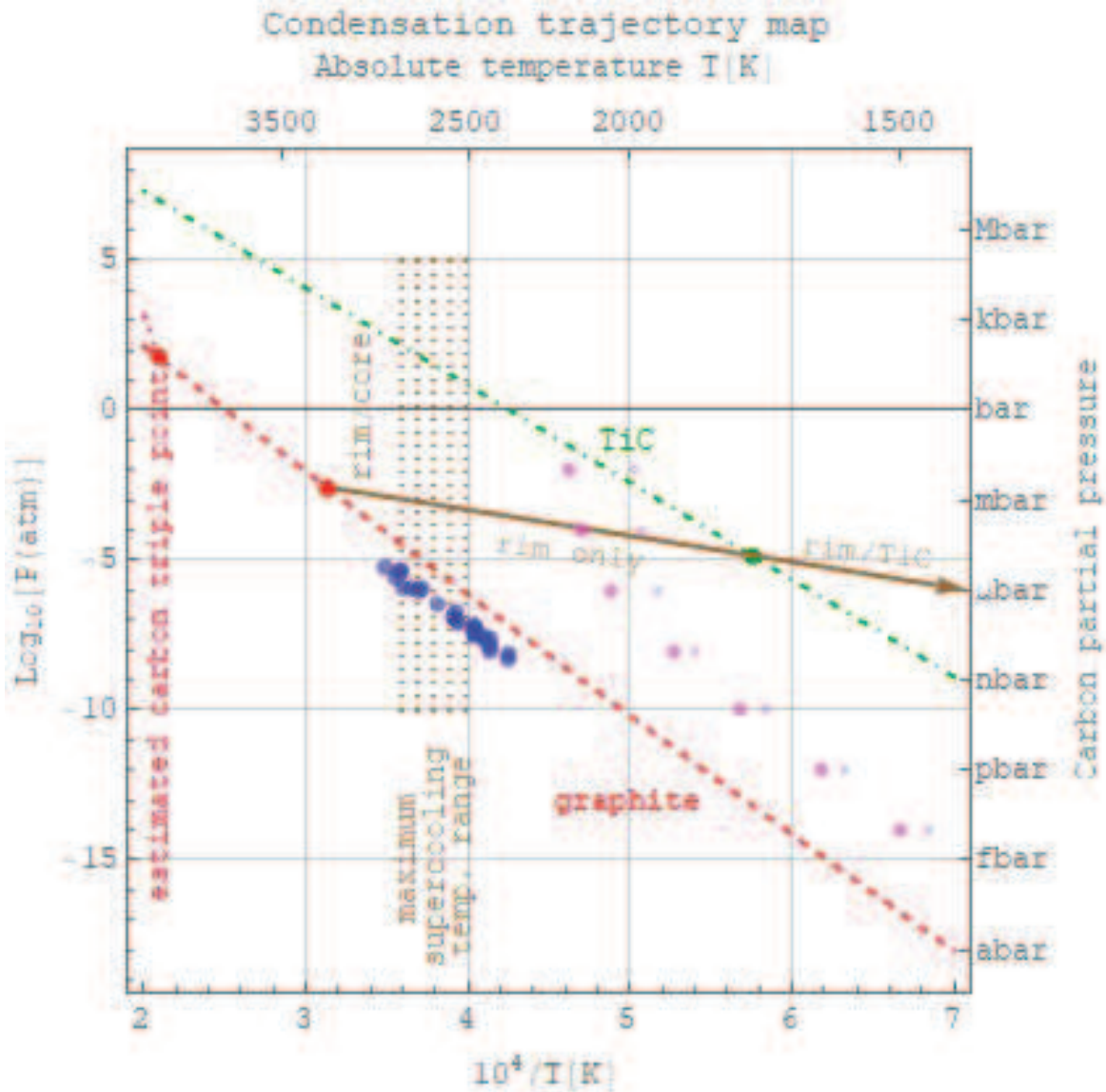


**Figure 4.** Sample condensation path (brown solid line running from left to right) for a parcel of C12-rich carbon which has been ejected into the photosphere of an AGB star from the s-process products layer, superposed on a  $\log[P]$  vs.  $1/T$  phase diagram. The red dashed line marks the partial pressure above which carbon vapor may condense just above blue data points from the classic Marshall & Norton (1950) paper, while the green dot-dashed line marks the pressure above which TiC may condense. Carbon vapor can condense and grow as liquid droplet particles only to the left of the dotted containerless maximum supercooling band, whose position remains to be experimentally determined. Between this band and the green dot-dashed line, the liquid droplets start growing graphite rims, and nucleation of new particles only happens on solid C clusters. To the right of the green line, the carbon vapor (depending on C/O ratio) may find preformed TiC "seeds" to condense upon instead. The seven magenta (and smaller indigo) dots mark changes to the red dashed carbon-condensation line when O/C goes from 0 up to 1/4 (and then 1/2) from Lodders & Fegley (1997). Thus oxygen may lower the condensation temperature to a point well below the "maximum supercooling temperature" for growth of liquid droplets.

spheres, argues for an origin near to the base of the very deep photosphere of these AGB stars, likely in convective eruptions of material from the s-process shell (Wasserburg et al. 1995). Those presolar carbon spheres which nucleate at a temperature below the maximum supercooling temperature for growth of a carbon droplet then appear to have nucleated on carbide seeds (if e.g. above the TiC line on Fig. 4) or homogeneously on a solid carbon seed. Home-grown onions nucleated on solid carbon in our "evaporating ovens" appear less compact, perhaps in part because of the anisotropic nature of graphite growth when not given a smooth (e.g. spherical substrate) for deposition. This is



consistent with our impression that the presolar core-rim particles are more abundant, than the rim-only and carbide-rim particles (Croat et al. 2003), in "high density" (KFC1) separates from the Murchison meteorite. Thus all three types of presolar graphite particle might be expected to originate under different conditions in the same type of stellar outflow.

From an astrophysics perspective, these observations suggest that the core of presolar core-rim carbon onions may permit: (i) an inventory of atoms heavier than carbon which have been trapped in the core since the solidification event in an AGB star atmosphere e.g. by aberration-corrected Z-contrast imaging (Pennycook 1989) say down to the 100 ppm level, and (ii) better core density measurements along with (iii) data on the laboratory conditions for unlayered graphene sheet nucleation and growth, to provide further insight into the astrophysical conditions of carbon droplet formation. Further computational model studies (currently underway cf. Lipp et al. (2017)) as well as laboratory studies of (iv) carbon-loop nucleation and abundance, (v) pair-correlation functions (e.g. by EXELFS), plus (vi) graphene sheet growth, interaction, and coherence-width (e.g. by electron diffraction and imaging), in slow-cooled carbon droplets may also provide further insight into practical possibilities for synthesis and use of this novel material.

## 5. CONCLUSION

Evaporation of carbon in the interior of a resistively-heated carbon rod shows promise for imitating the condensation of carbon in AGB star atmospheres. Observations so far indicate that a subset of carbon particles in presolar collections, with a graphite-rim/"unlayered-core" structure, condensed and grew initially as liquid droplets, perhaps deep within the topographically-complex photospheric surface (Freytag et al. 2017). Atoms heavier than carbon trapped on solidification (shown in Fig. 1b to be detectable by electron Z-contrast imaging) may have remained trapped throughout a large number of processes: Ejection from the star atmosphere by radiation pressure, interstellar travel to the site of collapse for our solar nebula, incorporation e.g. in the Murchison meteorite parent body about 4.5 billion years ago, collisional breakup of the parent body about 800,000 years ago (Caffee et al. 1988), atmospheric entry and impact in Australia in the late 1960's, dissolution of the meteorite at University of Chicago and slicing of the onions at Washington University several decades ago, as well as during 300 keV TEM work here and at Oak Ridge National Lab over the past two decades. On the materials side, both the presolar and the laboratory-specimen observations indicate that carbon vapor at low pressures condenses as liquid droplets, and if cooled slowly enough forms a network of atom-thick, unlayered and intersecting graphene sheets. If we can synthesize unlayered-graphene with the 4 nm coherence widths found in the presolar cores, the diffusion-barrier properties of intergrown-graphene may have applications on earth.

Thanks to WUSTls Bruce Fegley for insight into the literature and the carbon vapor pressure curve from the IVTAN thermodynamic database in Fig. 4, plus to Steve Pennycook for access to his 300kV Vacuum Generators 300keV Aberration-Corrected Scanning Transmission Electron Microscope at Oak Ridge National Laboratory in 2006, making possible the closeup of the core-rim interface in Fig. 1.

Work by TH was funded by award NNX15AK03H to the NASA Missouri Space Grant Consortium from the NASA Shared Services Center from the National Space Grant College and Fellowship Program within NASA's Office of Education, and further supported by UMSL Center for Nanoscience facilities access.

Author contributions: ML designed the first ovens, and characterized our first carbon onions. TH helped capture NASA-MO spacegrant funding for his work, and generated our core-rim and core-only onions and data therewith. PF helped out and also generated the first draft of the paper.

## APPENDIX

The material in this appendix is to outline supplementary data resources for this project. The work on laboratory synthesis is more recent, and in that context the sections below on "oven construction and use" and "electron microscopy" could be included in the manuscript if preferred.

However, in addition to electron microscope images and diffraction patterns from specimens synthesized in the laboratory, the conclusions in the paper draw also on years of work whose conclusions are published in Microscopy and Microanalysis proceedings papers, dissertations and an earlier ApJLett paper, but whose raw data has not. This latter data includes brightfield, diffraction, and electron phase contrast images of presolar core-rim carbon onions taken with our Philips EM430ST high resolution TEM, energy filtered TEM images for density analysis taken with a Zeiss microscope at the Danforth Plant Sciences Center in St. Louis, as well as aberration-corrected brightfield

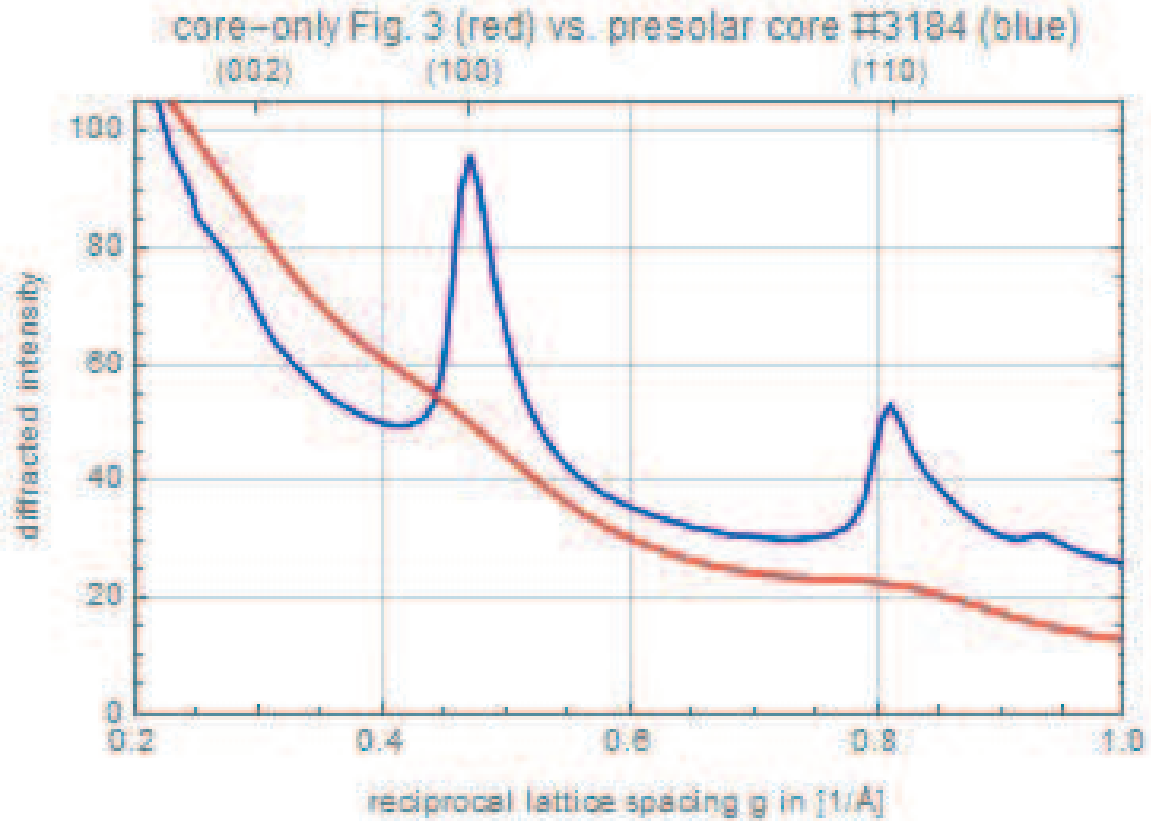


**Figure 5.** Comparing diffraction profiles of the “homemade” core-only particle profiled on the right side of Fig. 3, with the diffraction profile from the core-region of a presolar core-rim particle (Mandell et al. 2006), to show that the size and abundance of un-layered graphene sheets in the “homemade particles” is still much smaller than those found in the presolar cores.

and Z-contrast images taken of one specimen at Oak Ridge National Lab. Along with the metadata, these contain information that others might use to both to check our inferences and perhaps extract new information while the limited source of ultramicrotomed presolar “core-rim carbon onions” (e.g. from meteorites) is expanded in the years ahead.

The “additional data notes” section below only provides some examples of the kinds of analysis that can be done to compare such experimental data with models. We plan to create an on-line repository of raw data that may be useful to researchers (including links to archived versions of publications that are presently paywalled), but we can also offer some of it both to paper reviewers on request, as well to be published as part of the supplementary material resources for the paper.

## A. MATERIALS AND METHODS

### A.1. Oven construction and use

Our evaporating carbon ovens were manufactured in the lab using 6.2 mm diameter carbon rods cut into roughly 32 mm long segments. The oven consists of two segments: one segment is flat edged to collect the condensed carbon droplets and the other has a hole of diameter around 4 mm, made by drilling e.g. with a drill press, to a depth between 2 and 6 mm, followed by beveling of the hole sides down to a thin circular edge which will be pressed against the collection flat of the other segment, and which serves as the hottest part of the oven.

The two segments were then placed inside the standard carbon-evaporation holder of a Balzers turbo-pumped BAE 080 T vacuum evaporator. The ovens were heated using AC 5.6 volt electrodes through ovens with measured resistances between 0.9 and 0.3 ohm, to draw 35 to 104 watts of power for run times between 2 and 6 minutes. In one case we recorded the heat treatment using a Nikon 1 camera and neutral density filters to collect optical pyrometric data, and also recorded (generally over-exposed) 8-megapixel iSight camera movies to provide a record of events over time.



Debye powder diffraction profiles for flat graphene sheets of various sizes/shapes.

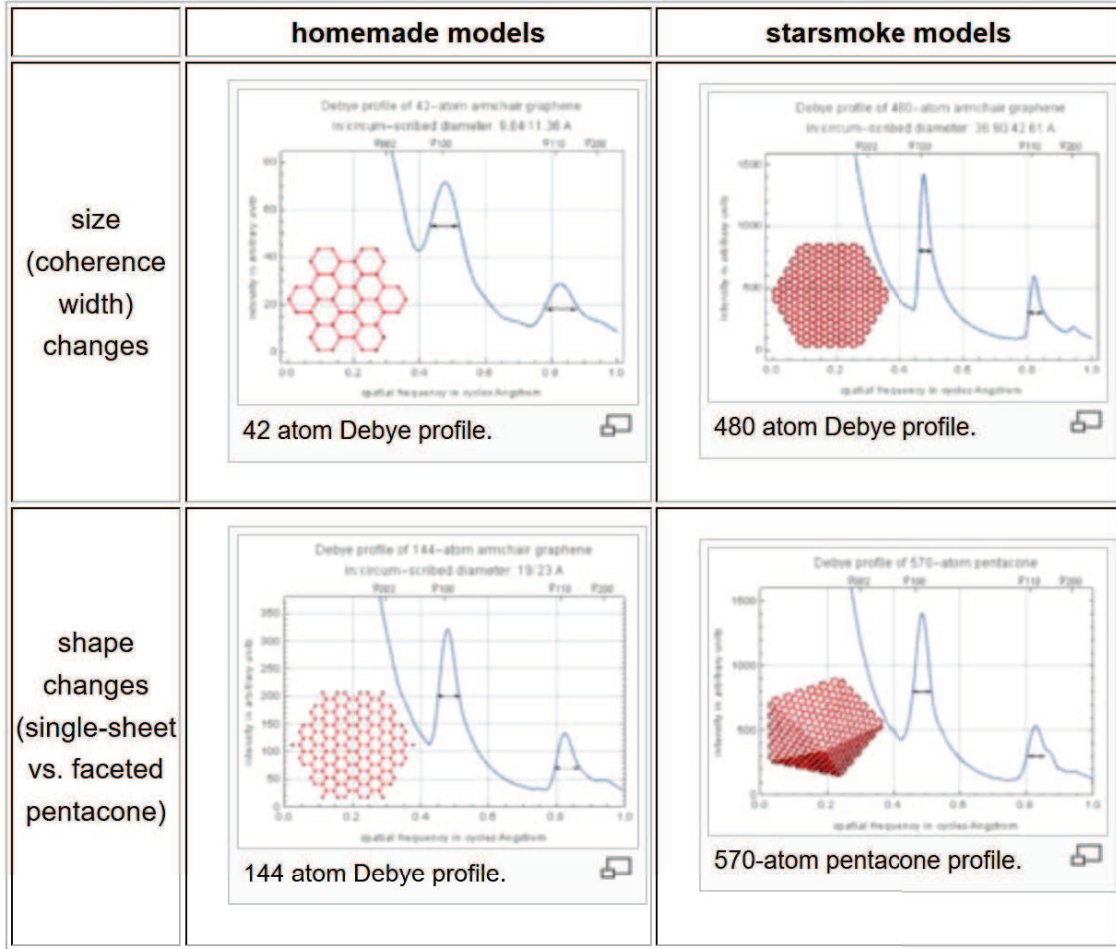


**Figure 6.** This comparison of graphite sheet size and shape effects on the “Debye scattering equation” diffraction profile average over all orientations (Warren 1969) were first applied to this problem by Mandell (2007).

### A.2. Electron microscopy

Transmission electron microscope (TEM) samples were removed from the ovens capture surface with a platinum loop, and deposited by direct contact onto a holey or lacey carbon TEM grid.

All of the transmission electron microscope (TEM) work reported here, except for the aberration-corrected brightfield/high-angle-annular-darkfield composite on the right side of Fig. 1, was taken with a TFS/FeiCo/Philips EM430 SuperTwin TEM operating at either 300 keV or 250 keV. Diffraction profiles were variously calculated and displayed with Semper6, ImageJ, and Mathematica.

### B. ADDITIONAL DATA NOTES

In Figures 5 and 6 we provide a comparison of electron diffraction profiles between a presolar core and the core-only particle shown in Fig. 3, and we provide some detail of the Debye scattering profile analysis (mentioned in the paragraph discussing coherence widths) to illustrate the effects of graphene sheet size and configuration on the diffraction profiles.

### REFERENCES

- Bernatowicz, T., Cowsik, R., Gibbons, P. C., Lodders, K., Jr., B. F., Amari, S., & Lewis, R. S. 1996, *Astrophysical Journal*, 760
- Bernatowicz, T. J., Akande, O. W., Croat, T. K., & Cowsik, R. 2005, *Astrophysical Journal*, 631, 988

- Bundy, F. P., a. Bassett, W., Weathers, M. S., Henley, R. J., Mao, H. U., & Goncharov, A. F. 1996, *Cargon*, 34, 141
- Caffee, M. W., Goswami, J. N., Hohenberg, C. M., Marti, K., & Reedy, R. C. Irradiation records in meteorites, ed. J. F. Kerridge M. S. Matthews, 205–245
- Croat, T. K., Bernatowicz, T., Amari, S., Messenger, S., & Stadermann, F. J. 2003, *Geochim. et Cosmochim. Acta*, 67, 4705
- Croat, T. K., Bernatowicz, T. J., & Daulton, T. L. 2014, *Elements*, 10, 441
- Croat, T. K., Stadermann, F. J., & Bernatowicz, T. J. 2005, *Astrophysical Journal*, 631, 976
- Fraundorf, P., Pisane, K., Mandell, E., & Collins, R. 2010, *Microscopy and Microanalysis*, 16, 1534
- Fraundorf, P. & Wackenhut, M. 2002, *Astrophysical Journal Letters*, 578, 153
- Freytag, B., Liljegren, S., & Hofner, S. 2017, *Astronomy and Astrophysics*
- Heer, W. A. D., Poncharal, P., Berger, C., Gezo, J., Song, Z. M., & Bettini, J. 2005, *Science*, 307, 907
- Hundley, T. J. & Fraundorf, P. 2018, in *Lunar and Planetary Science Conference*, 2154
- Kasuya, D., Yudasaka, M., Takahashi, K., Kokai, F., & Iijima, S. 2002, *J. Phys. Chem. B*, 106, 4947
- Kelton, K. F. & Greer, A. L. 2010, *Nucleation in Condensed Matter: Applications in Materials and Biology* (Amsterdam: Elsevier Science and Technology)
- Lipp, M., Savage, T., Osborn, D., & Fraundorf, P. 2017, *Microscopy and Microanalysis*, 23, 2192
- Lodders, K. & Fegley, B. in , *American Institute of Physics Conference Series*, ed. T. J. Bernatowicz E. Zinner, Vol. 402, 391–423
- Lugaro, M. 2005, *Stardust from meteorites: An introduction to presolar grains* (New York: World Scientific)
- Mandell, E. 2007, PhD thesis, University of Missouri - St. Louis and Rolla
- Mandell, E., Hunton, N., & Fraundorf, P. 2006, *Unlayered graphenes in red-giant starsmoke*, arXiv:cond-mat/060609
- Marshall, A. L. & Norton, F. J. 1950, *J. Am. Chem. Soc.*, 72, 2166
- Pennycook, S. J. 1989, *Ultramicroscopy*, 30, 58
- Savvatimskiy, A. 2015, *Carbon at high temperatures* (Amsterdam: Springer)
- Tielens, A. 2008, *Annual Review of Astronomy and Astrophysics*, 46, 289
- Warren, B. E. 1941, *Phys. Rev.*, 59, 963
- . 1969, *X-ray diffraction* (Reading MA: Addison-Wesley)
- Warren, B. E. & Bodenstein, P. 1966, *Acta Crystallographica*, 20, 602
- Wasserburg, G. J., Boothroyd, A. I., & Sackmann, I.-J. 1995, *Astrophysical Journal*, 447, L37
- Yang, C. C. & Li, S. 2008, *J. Phys. Chem.*, 112, 1423